

1 **Highly efficient transgenic mouse production using** 2 **piggyBac and its application to rapid phenotyping at** 3 **the founder generation**

4 **Eiichi Okamura^{1*}, Seiya Mizuno^{2*#}, Shoma Matsumoto^{1*}, Kazuya Murata², Yoko Tanimoto²,**
5 **Dinh Thi Huong Tra², Hayate Suzuki², Woojin Kang², Tomoka Ema², Kento Morimoto^{3, 4},**
6 **Kanako Kato², Tomoko Matsumoto⁵, Nanami Masuyama^{6, 7, 8}, Yusuke Kijima⁶, Toshifumi**
7 **Morimura¹, Fumihiro Sugiyama², Satoru Takahashi², Eiji Mizutani⁹, Knut Woltjen⁵, Nozomu**
8 **Yachie^{6, 8, 10, 11}, Masatsugu Ema^{1#}**

9 ¹ Department of Stem Cells and Human Disease Models, Research Center for Animal Life Science,
10 Shiga University of Medical Science, Otsu, Shiga, Japan

11 ² Laboratory Animal Resource Center, Trans-border Medical Research Center, University of Tsukuba,
12 Tsukuba, Ibaraki, Japan

13 ³ Doctoral Program in Medical Sciences, Graduate School of Comprehensive Human Sciences,
14 University of Tsukuba, Tsukuba, Ibaraki, Japan

15 ⁴ Research Fellow of the Japan Society for the Promotion of Science, Chiyoda-ku, Tokyo, Japan

16 ⁵ Department of Life Science Frontiers, Center for iPS Cell Research and Application (CiRA), Kyoto
17 University, Sakyo-ku, Kyoto, Japan

18 ⁶ School of Biomedical Engineering, Faculty of Applied Science and Faculty of Medicine, The
19 University of British Columbia, Vancouver, British Columbia, Canada.

20 ⁷ Institute for Advanced Biosciences, Keio University, Tsuruoka, Yamagata, Japan.

21 ⁸ Graduate School of Media and Governance, Keio University, Fujisawa, Kanagawa, Japan.

22 ⁹ Laboratory of Stem Cell Therapy, Faculty of Medicine, University of Tsukuba, Tsukuba, Ibaraki,
23 Japan

24 ¹⁰ Research Center for Advanced Science and Technology, The University of Tokyo, Meguro-ku,
25 Tokyo, Japan.

26 ¹¹ Premium Research Institute for Human Metaverse Medicine (WPI-PRIME), Osaka University,

27 Suita, Osaka, Japan

28 * These authors contributed equally to this work.

29

30 #Correspondence should be addressed to:

31 Seiya Mizuno, Laboratory Animal Resource Center, Trans-border Medical Research Center,

32 University of Tsukuba, Tsukuba, Ibaraki 305-8575, Japan

33 Tel.: +81-29-853-3393

34 Email: konezumi@md.tsukuba.ac.jp

35

36 Masatsugu Ema, Shiga University of Medical Science, Seta, Tsukinowa-cho, Otsu, Shiga 520-2192,

37 Japan

38 Tel.: +81-77-548-2334

39 Email: mema@bella.shiga-med.ac.jp

40 **Abstract**

41 Pronuclear microinjection is the most popular method for producing transgenic (Tg) animals.
42 Because the production efficiency is typically less than 20%, phenotypic characterization of Tg
43 animals is generally performed on the next generation (F₁) onwards. However, apart from in rodents,
44 in many animal species with long generation times, it is desirable to perform phenotyping in the
45 founder (F₀) generation. In this study, we attempted to optimize a method of Tg mouse production to
46 achieve higher Tg production efficiency using piggyBac transposon systems and established optimal
47 conditions under which almost all individuals in the F₀ generation were Tg. We also succeeded in
48 generating bacterial artificial chromosome Tg mice with efficiency of approximately 70%. By
49 combining this method with genome editing technology, we established a new strategy to perform
50 phenotyping of mice with tissue-specific knockout using the F₀ generation. Taking the obtained
51 findings together, by using this method, experimental research using Tg animals can be carried out
52 more efficiently.

53 **Keywords:** transgenic, piggyBac, transposon, conditional knockout

54 **Introduction**

55 Transgenic (Tg) technology enables genetic engineering techniques to introduce foreign DNA
56 sequences, namely transgenes from other species or artificial ones, into the genomes of organisms.
57 This technology can be used to produce organisms that express useful traits, such as resistance to
58 infectious diseases, a high growth rate, and herbicide resistance. In the medical field, Tg technology
59 has also made significant contributions, including the creation of disease model animals and the
60 elucidation of gene function¹⁻⁴. Another method for inserting foreign DNA into the genome is the
61 knock-in (KI) approach, which involves inserting foreign genes into specific targeted locations, in
62 contrast to Tg technology in which genes are inserted into the genome at random. Although KI
63 technology has the advantage of being able to perform genetic modification in a predictable manner,
64 it is generally inefficient and has difficulty introducing large-sized DNA. These problems with KI
65 technology are being overcome in some animals such as mice and rats via the development of
66 genome editing technology⁵⁻⁷. However, Tg technology is still considered useful for introducing
67 foreign genes into large animal species, including rabbit, pig, cattle, and non-human primates,
68 because efficient KI technology for such purposes has not yet been established.

69 The first Tg animal reported globally was a Tg mouse created by Jaenisch and Mintz in the
70 1970s⁸. A retrovirus was used as a vector for producing this mouse, but the transgene was not
71 expressed persistently due to silencing. In 1980, a pronuclear microinjection method, which is
72 currently the most popular technique for producing Tg mice, was reported⁹. However, the efficiency
73 of generating Tg mice using this method is approximately 20% at best¹⁰. Therefore, obtaining
74 enough Tg mice in the F₀ generation is difficult, and thus phenotypic analysis is generally performed
75 using animals from the next generation onwards. The efficiency of Tg animal production should thus
76 be improved in order to enhance research efficiency and to reduce the number of animals used, from
77 the perspective of animal welfare. A more efficient method for generating Tg mice is a method using
78 lentivirus first reported in 2003¹¹, in which Tg mice can be produced with approximately 80%–100%
79 efficiency. However, the lentiviral method is associated with the limitation that it can introduce
80 transgenes of approximately 8 kbp at most.

81 Another method for generating Tg animals is the transposon-based method. Transposons are
82 DNA sequences that can move from one location to another within the genome of an organism, and
83 were originally found in maize¹². During the transposition, the transposase enzymes bind to the
84 inverted terminal repeats (ITRs) that define the boundaries of the transposon and cut out the DNA
85 sequence between ITRs from the genome and insert it into another location. Several
86 transposon-based methods have been established and used to produce Tg animals, including Tol2¹³,
87 Sleeping Beauty¹⁴, and the piggyBac¹⁵ system. Transposon-based methods can introduce large
88 transgenes of 100 kbp or more, but the Tg production efficiency is generally less than 45%¹⁶, which
89 is lower than for the lentiviral method.

90 Recent developments in genome editing technology have made it possible to very efficiently
91 produce systemic knockout (KO) animals, in which large-scale phenotypic screening analysis at the
92 F₀ generation can be conducted¹⁷. Approximately 23% of gene KOs result in embryonic lethality¹⁸, in
93 which case tissue-specific KOs are often required to explore gene functions in a given tissue.
94 However, the establishment of tissue-specific Cre Tg mice and flox mouse strains is time-consuming
95 and laborious. Although many such mouse strains have been created and useful bioresources have
96 been established, tissue-specific KO often takes more than a year to obtain, cross, and finally obtain
97 the next generation for phenotypic analysis. Therefore, several methods have been reported to
98 perform tissue-specific KO in a single generation^{19–25}, but each method has its own advantages and
99 disadvantages, and thus they should be used appropriately depending on the purpose.

100 Here, we report a novel strategy for generating tissue-specific KO called ScKiP (single-step
101 cKO mouse production with piggyBac). We increased the efficiency of generating Tg mice with the
102 piggyBac transposon system by optimizing the method to deliver transposase and donor DNA into
103 the mouse zygote, and succeeded in producing Tg mice with an efficiency of nearly 100%. This
104 method even enabled us to introduce an approximately 170 kbp bacterial artificial chromosome
105 (BAC) vector with an efficiency of approximately 70%. By using this more efficient method, we
106 succeeded in establishing a new approach to performing tissue-specific KO at the F₀ generation. This
107 approach is expected to contribute to animal welfare by reducing the number of animals used and

108 also improve the efficiency of research.

109 **Materials and methods**

110 **Study approval**

111 All animal experiments were carried out in accordance with the Fundamental Guidelines for Proper
112 Conduct of Animal Experiments and Related Activities in Academic Research Institutions under the
113 jurisdiction of the Ministry of Education, Culture, Sports, Science and Technology, and Guidelines
114 for Proper Conduct of Animal Experiments from the Science Council of Japan. All animal
115 experimental procedures were approved by the Animal Care and Use Committee of Shiga University
116 of Medical Science (2020-6-21) and the Institutional Animal Experiment Committee of the
117 University of Tsukuba (22-019).

118

119 **Mice**

120 C57BL/6J and ICR mice were purchased from Charles River Laboratories (Yokohama, Japan).
121 PWK/Phj mice (RBRC00213) were obtained from RIKEN BioResource Research center (Tsukuba,
122 Japan). The mice were maintained in plastic cages under pathogen-free conditions in a room
123 maintained at $23.5 \pm 2.5^\circ\text{C}$ and $52.5 \pm 12.5\%$ relative humidity under a 14 h light:10 h dark cycle.

124

125 **Establishment of CdEC flox mouse line**

126 We selected a sequence (5'-CGC CCA TCT TCT AGA AAG AC-3') located in the first intron of the
127 *Gt(ROSA)26Sor* as the CRISPR target. Briefly, an expression cassette consisting of CAG promoter,
128 floxed EGFP, and Cas9NmC was placed between the 5'-homology arm and the 3'-homology arm. A
129 rabbit beta-globin polyadenylation signal sequence was placed downstream of each of floxed EGFP
130 and Cas9NmC. Cas9NmC is a fusion protein of Cas9 and part of mouse Cdt1 that we previously
131 reported²⁶. The CRISPR–Cas9 ribonucleoprotein complex and donor DNA were microinjected into
132 zygotes of C57BL/6J mice, in accordance with our previous report²⁷. Subsequently, microinjected
133 zygotes were transferred into the oviducts of pseudopregnant ICR female and newborns were
134 obtained. Genotyping for confirmation of the KI allele and random integration allele was performed

135 using the same methods as in our previous report²⁶. The CdEC flox mouse line was deposited to
136 RIKEN BioResource Research center (RBRC12114).

137

138 ***In vitro* fertilization, electroporation, and microinjection**

139 Fertilized eggs were obtained by *in vitro* fertilization using a method described elsewhere²⁸. Briefly,
140 oocytes were collected from oviducts of 10–14-week-old C57BL/6J females superovulated by the
141 intraperitoneal administration of CARD HyperOva (Kyudo, Tosu, Japan), followed by human
142 chorionic gonadotropin (hCG). Sperm were collected from the caudal epididymis of 12–16-week-old
143 C57BL/6J males, and then preincubated in Fertiup Mouse Sperm Preincubation Medium (Kyudo).
144 Insemination was performed in CARD medium (Kyudo), followed by incubation at 37 °C in an
145 atmosphere containing 5% CO₂ for 3 to 6 h. Fertilized eggs were washed to remove cumulus cells
146 and sperm, and incubated in KSOM medium (Ark Resource, Kumamoto, Japan) until
147 electroporation. Electroporation of fertilized eggs was performed in Opti-MEM I medium containing
148 piggyBac mRNA using Super Electroporator NEPA21 (Nepa Gene, Ichikawa, Japan) as described
149 elsewhere²⁹ with minor modifications. In this study, the poring pulse was set as follows: 225V, 2 ms
150 pulse width, 50ms pulse interval, 4 pulses, 10% attenuation rate, and + polarity. Meanwhile, the
151 transfer pulse was set as follows: 20V, 50ms pulse width, 50ms pulse interval, 5 pulses, 40%
152 attenuation rate, and ± polarity. The eggs were incubated until pronuclei were clearly visible. The
153 transposon DNA was microinjected under a microscope equipped with a micromanipulator and
154 Femtojet (Eppendorf, Hamburg, Germany). The injected one-cell embryos were cultured in KSOM
155 medium until the two-cell stage and then transferred into pseudopregnant ICR mice.

156

157 ***In vitro* transcription**

158 The template plasmid for piggyBac transposase (mPBase) for *in vitro* transcription was made by
159 replacement of a mouse codon-optimized mPBase cDNA sequence with an EGFP sequence of
160 pcDNA3.1-EGFP-poly(A)³⁰. After linearization of this template plasmid using XhoI restriction
161 enzyme, mPBase mRNA was synthesized using the mMACHINE T7 ULTRA

162 Transcription Kit (AM1345; Thermo Fisher Scientific, Waltham, MA, USA) or mMACHINE
163 mMACHINE T7 Transcription Kit (AM1344; Thermo Fisher Scientific).

164

165 **BAC DNA recombination**

166 A BAC DNA clone (RP24-125B24) containing the mouse *Flkl1* locus was obtained from Invitrogen
167 (Invitrogen, Carlsbad, CA, USA). Modification of the BAC DNA to insert the GFP sequence into the
168 first exon of the *Flkl1* gene was performed in a previous study^{31,32}. To insert ITR (inverted terminal
169 repeat) sequences and Kusabira-Orange expression cassette into the backbone vector region, the
170 BAC DNA was further modified by the same method as described in that previous study³¹ using the
171 RED/ET recombination technique (Gene Bridges, Heidelberg, Germany). Collected recombinants
172 were identified by screening for kanamycin resistance, followed by PCR analysis. The PGK-gb2-neo
173 expression cassette was not excised.

174

175 **Genotyping of the embryo**

176 E11.5 (embryonic day 11.5) stage embryos were collected from the uteri of surrogate mothers after
177 euthanasia and the placenta and yolk sac were removed. The fluorescent signal was captured under a
178 fluorescent stereoscopic microscope (FL5; Leica Microsystems, Wetzlar, Germany) equipped with a
179 camera (DP73; Olympus, Shinjyuku, Japan). Genomic DNA from the embryos was extracted by
180 phenol/chloroform extraction. Genotyping PCR was performed using a primer set to detect the GFP
181 sequence using conventional PCR (T100; Bio-Rad, Hercules, CA, USA). To determine the copy
182 number of the transgene, droplet digital PCR (ddPCR) was performed using the Qx200 Droplet
183 Digital PCR system (Bio-Rad) with the GFP and Tfrc Primer/Probe set.

184

185 **Southern blotting**

186 Genome DNA was extracted from mouse embryos with phenol and chloroform, and then purified by
187 ethanol precipitation. After the digestion of 5 μ g of genomic DNA by EcoRI, the concentration was
188 measured using a Quantus Fluorometer (Promega, Madison, WI, USA). One microgram of digested

189 DNA was electrophoresed in 1% agarose gel. The DNA was blotted onto a nylon membrane
190 (Amersham Hybond-N⁺; GE Healthcare, Chicago, IL, USA) and hybridized with DIG-labeled probe
191 using DIG Easy Hyb (Roche Diagnostics, Mannheim, Germany). Salmon sperm DNA was used in
192 the blocking step. After the reaction with anti-digoxigenin-AP Fab fragments (Roche), the bands
193 were detected by enhanced chemiluminescence using CDP-Star (Roche) and ImageQuant LAS 4000
194 Mini (GE Healthcare). All probes were synthesized by PCR using DIG DNA Labeling Mix, 10×
195 Conc. (Roche).

196

197 **Inverse PCR**

198 PCR was performed using a method described elsewhere³³ with minor modifications. In this study,
199 3μg of DNA was digested by EcoRI and the digested DNA was self-ligated using DNA Ligation Kit
200 (Mighty Mix; Takara Bio, Kusatsu, Japan) after purification by ethanol precipitation. Regions where
201 transgenes became integrated were amplified using transgene-specific primers by shuttle PCR.
202 Nested PCR was also performed to enrich the genomic regions of interest.

203

204 **Echocardiography**

205 A Vevo 2100 High-Resolution Imaging System (Visual Sonics Inc, Toronto, ON, Canada) was used
206 to evaluate cardiac contractility. Mice were anesthetized with 2.5% isoflurane in oxygen and placed
207 on a warmed platform. The isoflurane concentration was maintained at 1.5% during imaging. An
208 ultrasound gel was applied to the left anterior thorax after the removal of fur from the body.
209 Short-axis M-mode images were obtained at the level of the papillary muscle using a 40-MHz
210 transducer. Left ventricular end-diastolic diameter (LVEDD) and left ventricular end-systolic
211 diameter (LVESD) were measured using Vevo LAB software (FUJIFILM Visualsonics, Toronto, ON,
212 Canada). Fractional shortening (FS) was calculated at three different time points of each mouse as
213 follows: $FS (\%) = (LVEDD - LVESD) / LVEDD \times 100$.

214 **Results**

215 **piggyBac transgenesis by electroporation and pronuclear microinjection**

216 Although previous works achieved considerably high efficiency in the generation of Tg mice¹⁵, we
217 assumed that Tg mice could be generated with even higher efficiency by initiating the expression of
218 mammalian codon-optimized mPBBase at an earlier timing than in the previous methods. To test this,
219 we introduced *in vitro*-synthesized mPBBase mRNA into zygotes by electroporation early after *in*
220 *vitro* fertilization (Figure 1a). Consistent with previous reports describing that excessive amounts of
221 mPBBase inhibit transposition activity, a phenomenon called overproduction inhibition (OPI), we
222 confirmed that OPI occurred at a high dose of mPBBase in mouse ES cells, by varying the amount of
223 mPBBase expression plasmid with a certain amount of donor plasmid DNA (Figure 1b). To optimize
224 the concentration of mPBBase mRNA for electroporation, we applied it at 0, 20, 100, and 500ng/ μ l.
225 After electroporation, the fertilized eggs were cultured *in vitro*, and donor plasmid DNA containing a
226 GFP expression cassette (Figure 1c) was microinjected into the pronucleus at the PN3–4 stage
227 (Figure 1a). Those embryos were cultured *in vitro* until the E4 stage. We counted the blastocysts
228 exhibiting GFP fluorescence under each set of conditions by fluorescence microscopy and found that
229 conditions with 500ng/ μ l mRNA gave the best results, at which approximately 80% of the
230 blastocysts exhibited fluorescence (Figure 1d, e). To confirm this result at a later developmental
231 stage, we transplanted two-cell-stage embryos into the oviduct of a surrogate mother, removed
232 embryos from the uterus at E11.5 and dissected them, and conducted fluorescence observation as
233 well as ddPCR to detect the transgene. The obtained results indicated that, for the 100ng/ μ l group, 9
234 out of 10 were Tg, while for the 500 and 1000ng/ μ l groups, all embryos were Tg. Although there
235 were no significant differences in copy number of the transgene among all groups, the 500ng/ μ l
236 group had the highest mean copy number (Figure 1f). From these results, we concluded that an
237 mRNA concentration of 500ng/ μ l is optimal to produce Tg mice.

238 To confirm that this method would result in healthy births, we transplanted the fertilized eggs
239 into surrogate mothers. We found that, out of 70 fertilized eggs, 12 (17%) animals were born; of

240 these, 1 animal was eaten by its mother, while the rest of them (11 animals) were Tg (Figure 1g). To
241 evaluate the reproductive ability of the F₀ generation, three males were mated and all resulting
242 offspring were found to be Tg (Figure 1h).

243

244 **Bacterial artificial chromosome DNA integration by piggyBac transposase**

245 Relatively short plasmids were used as the donor DNA in our assay, and therefore we attempted to
246 use larger donor DNAs with several expression cassettes. We constructed two plasmids with a larger
247 12kbp transgene. One was a construct containing an expression cassette for GFP-P2A-mCherry
248 linked to the Ubiquitin C promoter (Figure 1i). All eight E11.5 embryos showed GFP and mCherry
249 expression (Figure 1j). The other was a construct containing expression cassettes for GFP linked to
250 the *Myh6* promoter and tdTomato linked to the CAG promoter (Figure 1k). We obtained four
251 embryos that reached the E9.5 stage, seven that reached E11.5, and three newborns, all of which
252 showed tdTomato expression (Figure 1l&m). We also confirmed heart-specific GFP expression in all
253 of the embryos at E9.5 and E11.5 by fluorescence microscopy (Figure 1l&n). Finally, ddPCR was
254 performed using DNAs extracted from E11.5 embryos to analyze the transgene copy number. The
255 results revealed 9.7 ± 8.6 , and 5.8 ± 3.3 copies of the transgenes in UbC pro.-GFP-P2A-mCherry and
256 *Myh6* pro.-GFP-CAG-tdTomato mice, respectively (Figure 1o).

257 Mice of 12kbp Tg were established at 100% efficiency, and therefore we applied this method to
258 establish BAC Tg mice because the efficiency of BAC Tg mouse production is typically very low. In
259 a previous study, we constructed BAC DNA with a GFP sequence linked to the *Flk1* promoter. Here,
260 the ITR sequences and Kusabira-Orange cassette were inserted into the vector backbone of the BAC
261 DNA (Figure 1p). The engineered BAC DNA was used as a donor DNA at two different
262 concentrations (1 and 10ng/ μ l). Owing to the high viscosity of BAC DNA, microinjection at
263 concentrations higher than 10ng/ μ l was not feasible. We obtained 14 Tg animals out of 19 embryos
264 at E11.5 under conditions with 1ng/ μ l, while 7 out of 10 embryos were Tg at E11.5 under conditions
265 with 10ng/ μ l only when mPBase had been introduced (Figure 1q). Thus, there was no significant
266 difference in the percentage of Tg mice under the two sets of conditions. Next, we evaluated the

267 transgene copy number in these Tg mice by ddPCR and found that the mean copy numbers were
268 0.39 and 2.39 for 1 and 10ng/ μ l, respectively, which were significantly different (Figure 1r). The
269 BAC Tg embryos exhibited ubiquitous Kusabira-Orange expression throughout the body and
270 specific GFP signals in the blood vessels (Figure 1s), consistent with a previous report³¹. Finally,
271 PCR genotyping analysis indicated that the percentage of Tg mice among the offspring was very
272 high (52 out of 94; 55%).

273

274 **Donor DNA injection into fertilized eggs refrigerated after electroporation**

275 Although the method using electroporation and microinjection developed in this study can produce
276 Tg mice with very high efficiency, the experimental schedule is inconvenient due to microinjection
277 being performed late at night. Therefore, we modified the schedule by storing the eggs after
278 electroporation in a fridge, and then performed microinjection the next morning (Figure 2a). After
279 either a mixture of BFP/EGFP/tdTomato expression vectors (three colors) or a mixture of
280 BFP/EGFP/tdTomato/E2Crimson (four colors) (Figure 2b) was microinjected, the fertilized eggs
281 were transplanted into the oviduct of surrogate mothers at the one-cell stage. We dissected the
282 embryos at E14.5 and checked the presence of fluorescence as an indicator of Tg. We obtained 12
283 embryos, 11 (91.7%) of which were Tg under the three-color conditions, while 3 out of 4 embryos
284 (75%) were Tg under the four-color conditions (i.e., at least one fluorescence signal was shown)
285 (Figure 2c&d). These results indicate that Tg mice can be generated at high efficiency even after
286 refrigeration of the fertilized eggs.

287

288 **Rapid phenotyping of conditional KO mice at the F₀ generation by ScKiP**

289 Currently, for phenotypic analysis of essential genes in a certain tissue that play roles in embryonic
290 survival, the Cre-loxP system must be used, which is time-consuming and laborious. By using the
291 method established in this study, we attempted to establish a new strategy to generate conditional
292 KO at the F₀ generation by using piggyBac transgenes. First, we targeted the *Prmt1* gene, which
293 causes dilated cardiomyopathy of young mice upon heart-specific KO, while its systemic KO is

294 embryonically lethal³⁴. For heart-specific KO, we constructed a donor plasmid with the Cre gene
295 linked under a cardiac-specific *Myh6* promoter and a gRNA for the *Prmt1* gene expression cassette
296 (Figure 3a). Prior to the conditional KO experiment, to check that the *Myh6* promoter causes Cre
297 expression in the heart, we produced Tg mice in the GRR mouse³⁵ strain background. The GRR
298 allele has a structure in which the floxed EGFP-polyA sequence and the tdTomato gene are linked
299 under the CAG promoter, and tdTomato is expressed following Cre-mediated excision (Figure 3b).
300 The donor plasmid was microinjected into the pronuclei after storage at 4°C overnight, and those
301 eggs were transplanted into the oviduct of a surrogate mother at the one-cell stage. We obtained 14
302 offspring, 10 of which were revealed to possess the transgene (GRR KI/Tg+) by genotyping PCR
303 analysis. Fluorescent microscopy of the born mice indicated that most of the GRR KI/Tg+ mice
304 showed strong tdsRed fluorescence in the heart, along with nonspecific expression in regions
305 including the skin (Figure 3c&d). To perform conditional KO, we used the CdEC flox mouse strain
306 containing the KI allele in which the floxed EGFP-polyA sequence and the Cas9NmC gene are
307 linked under the CAG promoter, and Cas9NmC is expressed only after Cre expression (Figure 3e).
308 Tg mice with the same donor vector were produced in a similar way in the CdEC flox mouse strain.
309 The results revealed that 10 offspring were obtained, and genotyping PCR analysis revealed that all
310 animals possessed the CdEC flox KI allele, while only one had the transgene (CdEC KI/Tg+).
311 Echocardiography at 2, 4, and 6 weeks old revealed that cardiac contractility of the CdEC KI/Tg+
312 mouse was reduced compared with that in mice without transgene (CdEC KI/Tg-, Figure 3f). At 50
313 days old, we noticed that the CdEC KI/Tg+ mouse was sluggish and wheezed, and thus euthanized it.
314 The heart of this CdEC KI/Tg+ mouse weighed 188mg, which was markedly heavier than that of a
315 CdEC KI/Tg- mouse (101mg, Figure 3g), suggesting dilated cardiomyopathy similar to that of
316 conventional cKO mice reported previously³⁴. Thus, although we were able to observe a phenotype
317 of heart-specific KO of the *Prmt1* gene at the F₀ generation, the rate of Tg mice relative to all
318 offspring was low at 10% in this experiment. This may have been due to ectopic Cre expression
319 other than in the heart in Tg embryos, resulting in embryonic lethality.

320 Given the success of characterizing the heart-specific phenotype associated with *Prmt1*, we

321 applied this strategy to characterize mice with germ cell-specific KO of the *Kit* gene at the F₀
322 generation. It has been reported that mice with hypo-functional *Kit* point mutant (*W^v/W^v*) had no
323 sperm, while systemic KO with deletion of the transmembrane domain (*W/W*) resulted in perinatal-
324 or late fetal-stage lethality. To avoid lethality due to non-specific Cre-loxP recombination, we used
325 germ cell-specific *Ddx4* promoter-driven CreERT2, which works only in the presence of tamoxifen
326 as a component of the donor plasmid with an expression cassette of gRNA for the *Kit* gene (Figure
327 3h). Similar to the procedure in the previous experiment, after mPBac introduction into fertilized
328 eggs prepared using CdEC flox KI male and wild-type female mice, the donor plasmid was
329 microinjected into the pronuclei, followed by transplantation into the oviduct of a surrogate mother
330 at the one-cell stage. We obtained 14 offspring, including 11 males and 3 females (Figure 3i), all of
331 which were revealed to have the transgene and KI allele (CdEC KI/Tg+) by genotyping PCR. Nine
332 males were used for subsequent experiments. From each of these nine males, one testis was removed
333 as a control (before tamoxifen sample) at 16 to 17 weeks old. Tamoxifen was injected three times at
334 18, 22, and 23 weeks old to induce Cre-loxP recombination. During this process, six mice died
335 probably due to tamoxifen toxicity, postoperative complications, or non-specific *Kit* gene KO in
336 cells other than germ cells. At 32 weeks old, the remaining three males were euthanized and their
337 testes were collected (after tamoxifen sample). HE-stained sections from the removed testes were
338 prepared and the proportion of seminiferous tubules not containing sperm heads was determined
339 (Figure 3j). It was found that the number of seminiferous tubules without sperm increased after
340 tamoxifen administration compared with that before tamoxifen administration in all three males
341 (Figure 3k). When the percentage of Cas9-expressing undifferentiated spermatogonia after
342 tamoxifen administration was examined by immunostaining using anti-Cas9 and anti-GFR α 1
343 antibody, reductions in undifferentiated spermatogonia (8.5%, 86%, and 59%) were seen in samples
344 No. 1, 2, and 3, respectively (Figure 3l). We named this cKO method “ScKiP,” which stands for
345 single-step cKO mouse production with piggyBac.

346

347 **Preference of the Tg integration site and parental alleles in mouse zygote**

348 To reveal the preference of integration sites into which Tg is introduced by our piggyBac system, we
349 prepared fertilized eggs with PWK/Phj (PWK) strain sperm and C57BL/6J (B6) strain oocyte, and
350 then injected mPBase mRNA and a donor plasmid DNA containing GFP and a DNA barcode
351 sequence (Figure 4a). We obtained 17 E11.5 embryos, 9 of which were Tg as judged by fluorescence
352 microscopy and genomic PCR. We investigated the number of integration sites in each Tg embryo
353 by Southern blotting (Figure 4b). We confirmed that one to three transgenes had integrated into
354 different genomic regions of the genome in each embryo. We further performed ddPCR analysis to
355 evaluate the copy number (Figure 4c). Subsequently, we detected the DNA barcode sequence of the
356 Tg by Amplicon-seq; overall, we detected 16 unique DNA barcode sequences. To investigate the
357 sites of integration of the Tg in the genome, we performed inverse PCR and confirmed the results by
358 genotyping PCR using primers specific for the DNA barcode sequence. Focusing on the genomic
359 features of the integration site, 9 out of 16 transgene were located in introns, 3 were in repeat
360 sequences, 3 were intergenic regions and only 1 was located coding sequence. (Figure 4d). Using
361 information on the SNPs between the PWK and B6 genomes, we could determine whether the
362 transgene was introduced into the paternal or maternal allele for 13 out of 16 transgenes (Figure 4e).
363 Overall, 3 transgenes were on the maternal allele, even though we injected donor DNA into the male
364 pronucleus. This suggested that the DNA integration event by mPBase continued after pronuclear
365 fusion. To obtain a deeper understanding of the integration sites, we performed comparative analysis
366 using ChIP-seq data. It was reported that the integration sites for mPBase were enriched in regions
367 with H3K4me3³⁶. We downloaded H3K4me3 ChIP-seq data of the zygote and early two-cell embryo
368 with PWK sperm and B6 oocyte from the GEO database, and compared the peaks with the
369 integration sites (GSE71434)³⁷. Overall, 31.25% of integration sites overlapped with H3K4me3,
370 which is generally located on the active TSS, for the integrated allele (Figure 4f, g).

371 Discussion

372 In this study, we established a highly efficient Tg production method using the piggyBac transposon
373 system. Three types of transposon systems are commonly used to create Tg animals: piggyBac,
374 Sleeping Beauty, and Tol2³⁸. Among them, we employed piggyBac because it is the only transposase
375 used to create Tg mice with transgenes larger than 150 kbp³⁹. By mPBase mRNA electroporation and
376 pronuclear donor DNA microinjection, a plasmid-sized transgene with 100% efficiency and a BAC
377 transgene with approximately 70% efficiency could be introduced.

378 Previous works indicated that the efficiency of Tg mouse production by mPBase was typically
379 20%–70%. The previously described methods and ours differ in terms of how mPBase is
380 introduced. In several previous studies, mPBase expression plasmid vector was introduced into the
381 cytoplasm of unfertilized eggs or the pronucleus of fertilized eggs^{15,40–42}. Urschits *et al.* showed that
382 mPBase protein expression was at the background level until 6 h after injection of the expression
383 plasmid, and peak expression was observed at about 30 h⁴⁰. Therefore, mPBase is fully expressed
384 after the two-cell stage, and donor plasmids introduced at the one-cell stage might be degraded or
385 diluted until the mPBase protein functions. In other reported studies, mPBase mRNA was used
386 instead of an expression plasmid, but it was injected at the pronuclear stage^{43–47}, and thus full
387 expression may have occurred after the two-cell stage. In contrast, in this study, we attempted to
388 introduce mPBase mRNA immediately after fertilization using electroporation. In this method,
389 mPBase was sufficiently expressed when donor DNA was injected into the pronucleus and the
390 transgene integration may have occurred efficiently before donor DNA degradation or dilution.

391 In this study, although we attempted to improve the efficiency of piggyBac transgenesis in mice,
392 improvement of Tg production efficiency is also useful for other animal species. In rat, another
393 popular experimental animal, pronuclear injection of a piggyBac expression plasmid vector and
394 donor DNA has been used to generate Tg animals, but the efficiency was generally less than
395 30%^{44,48,49}. Although a study reported that Tg rats can be produced more efficiently (33%–100%,
396 mean of nearly 80%) using mPBase mRNA pronuclear microinjection⁵⁰, it may be possible to
397 consistently produce Tg animals even more efficiently if mPBase mRNA is introduced at an earlier

398 timing after *in vitro* fertilization. Transgenic technology is also important for livestock, such as cattle,
399 pig, and sheep, but there are very limited reports on application of the piggyBac transposon system
400 to their zygotes^{51,52}. Somatic cell nuclear transfer is one of the most common methods to create Tg
401 livestock^{53,54}. However, this approach is technically difficult, and the birth rate is typically low.
402 Although no reports have yet been published on the use of mPBase mRNA injection to produce Tg
403 livestock, this approach is worth pursuing.

404 Mice with tissue-specific conditional KO are very useful to elucidate gene functions *in vivo* but
405 are time-consuming to produce because they typically require flox and Cre-Tg animal strains to be
406 obtained and crossed. Recently, new methods have been developed to perform tissue-specific KO in
407 a rapid manner. One example involves introducing CRISPR-Cas9 ribonucleoproteins into mice using
408 nanoparticles, which enables efficient KO in several tissues, including liver, muscle, brain, kidney,
409 and lung¹⁹⁻²². Another example involves introducing the flox allele into zygotes obtained from
410 tissue-specific Cre-Tg mice by KI technology²³. A third example involves the introduction of gRNA
411 by an adeno-associated virus (AAV) vector into tissue-specific Cas9-expression Tg mice. Finally, a
412 method has been developed involving the introduction of gRNA and a tissue-specific Cre expression
413 vector by AAV into mice harboring a Cre-loxP reaction-dependent Cas9 expression cassette.
414 Although these methods are very useful, they vary in terms of their targetable tissues, efficiency of
415 cKO generation, and procedural difficulty. Thus, it is important to carefully examine these options
416 and choose an appropriate method considering the purpose of the planned research. In this study, as
417 another option to perform cKO experiments within a short time, we developed the ScKiP method
418 and tested its usefulness. For rigorous evaluation, we selected *Prmt1* and *Kit* as target genes, for
419 which a cKO experiment is necessary to reveal their functions after birth because their systemic KO
420 is embryonically lethal. Although we confirmed that this method is not strictly tissue-specific,
421 probably due to positional effects, we could observe the expected phenotype. Therefore, the ScKiP
422 method is considered to be useful for rapid screening analysis of gene function. In addition, using the
423 ScKiP method, KO cells can be identified using the disappearance of EGFP fluorescence as an
424 indicator, which is a feature not found in other methods described above.

425 Taking the obtained findings together, by using the Tg production method that we have
426 established, we can obtain a sufficient number of animals for phenotypic analysis in the F₀
427 generation. Our methods are expected to contribute to animal welfare by reducing the number of
428 animals used and enabling research to be carried out more efficiently.

429

430 **Acknowledgments**

431 pcDNA3.1-EGFP-poly(A) plasmid was kindly provided by Dr. Kazuo Yamagata (KINDAI
432 University). This work was supported by JSPS KAKENHI Grant Numbers 21K05988, 23H03860 (to
433 E.O.), 20K22611 (to S.M.), and 21H02388 (to M.E.). We thank Central Research Laboratory at
434 Shiga University of Medical Science and Single-cell Genome Information Analysis Core (SignAC)
435 at WPI-ASHBi, Kyoto University, for their support. We also thank Edanz (<https://jp.edanz.com/ac>)
436 for editing a draft of this manuscript. Finally, we thank all members of the Department of Stem Cells
437 and Human Disease Models, Research Center for Animal Life Science, Shiga University of Medical
438 Science.

439 **Figure legends**

440 **Figure 1 Generation of Tg mice by mPBase mRNA electroporation and donor plasmid DNA** 441 **pronuclear microinjection**

442 (a) Schematic representation of the method to introduce mPBase mRNA and donor plasmid DNA.
443 Typical schedule for performing each procedure is shown at the top of the figure. (b) Donor plasmid
444 introduction into the ES cell genome using the piggyBac transposon system. ES cells were
445 transfected with different concentrations of the mPBase expression plasmid vector and the same
446 concentration of the donor plasmid, and the number of puromycin-resistant colonies was counted. (c)
447 Schematic representation of CAG-EGFP-IRES-Puro donor plasmid DNA. Only the region between
448 two ITRs is described. (d, e) Investigation of the optimal concentration of mPBase mRNA by
449 observing blastocyst embryos using fluorescence microscopy. Fluorescence microscopic images of
450 conditions with mRNA at 0 and 500ng/ μ l are shown in d. Tg embryos were judged by the presence
451 of GFP fluorescence (orange arrow: GFP positive, white arrow: GFP negative blastocysts), with
452 GFP-positive rates being displayed as a bar graph in e. Blue dots indicate blastocyst development
453 rates for the number of fertilized eggs tested. (f) Investigation of the optimal concentration of
454 mPBase mRNA using DNAs from E11.5 embryos. Transgene copy numbers were determined by
455 ddPCR for the GFP sequence. (g) Fluorescent image of born Tg mice at the P1 (postnatal day 1)
456 stage. (h) A mating test was performed to confirm germline transmission of the transgene. Three Tg
457 male mice (#8, #9, #10) were crossed with wild-type (WT) females; the pedigree of line #8 is shown.
458 Regarding line #8, copy numbers of the transgene were determined by ddPCR using DNA obtained
459 from the tail tip. The numbers in black boxes indicate the copy numbers of the transgene determined
460 by ddPCR using tail-derived DNA from F₀ and F₁ animals. (i) Schematic representation of UbC
461 pro.-GFP-P2A-mCherry donor plasmid DNA. Only the region between two ITRs is described.
462 cHS4: chicken hypersensitive site-4 insulator element. (j) Fluorescent images of E11.5 embryos
463 harboring UbC pro.-GFP-P2A-mCherry transgene. Bright field (left), GFP fluorescence (middle),
464 and mCherry fluorescence images (right) are shown. (k) Schematic representation of Myh6
465 pro.-GFP-CAG-tdTomato donor plasmid DNA. Only the region between two ITRs is described. (l)

466 Fluorescent images of representative E9.5 embryos harboring Myh6 pro.-GFP-CAG-tdTomato
467 transgene. Bright field image taken using a stereomicroscope (left), tdTomato fluorescence (2nd from
468 left), GFP fluorescence (2nd from right), and merged images (right) taken using a confocal
469 microscope are shown. (m) Fluorescent images of E11.5 embryos harboring Myh6
470 pro.-GFP-CAG-tdTomato transgene. Bright field (left) and tdTomato fluorescence images (right) are
471 shown. (n) Confocal microscopic images of representative E11.5 embryos harboring Myh6
472 pro.-GFP-CAG-tdTomato transgene. Transverse frozen sections were prepared. Bright field image
473 taken using a phase contrast microscope (upper left), tdTomato fluorescence (upper right), GFP
474 fluorescence (lower left), and merged images (lower right) taken using a confocal microscope are
475 shown. (o) Copy number analysis of Tg embryos harboring UbC pro.-GFP-P2A-mCherry transgene
476 (UbC) and Myh6 pro.-GFP-CAG-tdTomato transgene (Myh6). (p) Schematic representation of BAC
477 DNA used as a donor vector. (q) Investigation of the optimal concentration of donor DNA using
478 DNAs from E11.5 embryos. Transgenes were detected by conventional PCR and GFP-positive rates
479 are displayed as a bar graph. Blue dots indicate E11.5 development rates for the number of
480 transplanted two-cell-stage embryos. (r) Copy number analysis of BAC Tg. Transgene copy numbers
481 were determined by ddPCR for the GFP sequence using DNAs from E11.5 embryos. (s) Fluorescent
482 images of a representative E11.5 BAC Tg embryo. Bright field (left), Kusabira-Orange fluorescence
483 (middle), and GFP fluorescence images (right) of the whole body (top), head (middle), and somite
484 (bottom) region are shown. The red rectangular frames inside the whole body represent the head and
485 somite region.

486

487 **Figure 2 Generation of Tg mice using fertilized eggs refrigerated after electroporation**

488 (a) Schematic representation of method to introduce mPBase mRNA and donor plasmid DNA.
489 Fertilized eggs were temporarily refrigerated after electroporation. Typical schedule for performing
490 each procedure is shown at the top of the figure. (b) Schematic representation of BFP, EGFP,
491 tdTomato, and E2Crimson expression cassettes on the donor plasmids. (c) Summary of the results of
492 observing the obtained embryos by fluorescence microscopy. The presence of each fluorescence

493 color is indicated by + and its absence is indicated by -. The results of three- (top) and four-color
494 donor plasmid injection (bottom) are shown separately. (d) Fluorescent images of representative
495 E11.5 embryo harboring four-color transgenes. BFP (left), EGFP (2nd from left), tdTomato (2nd from
496 right), and E2Crimson fluorescent images (right) are shown.

497

498 **Figure 3 Rapid phenotyping of conditional KO mice**

499 (a) Schematic representation of Myh6-Cre-Prmt1 gRNA donor plasmid DNA. Only the region
500 between two ITRs is described. cHS4: chicken hypersensitive site-4 insulator element. pA:
501 polyadenylation signal. (b) Schematic representation of GRR KI allele. (c) Fluorescent images of
502 born GRR KI mice with Myh6-Cre-Prmt1 gRNA transgene (GRR KI/Tg⁺) at the P4 (postnatal day
503 4) stage. Fluorescent image of GRR KI mice without the transgene (GRR KI/Tg⁻) was shown as a
504 control. (d) Fluorescent images of heart from GRR KI/Tg⁺ and GRR KI/Tg⁻ mice. (e) Schematic
505 representation of CdEC flox KI allele. (f) Results of echocardiography on 2-, 4-, and 6-week-old
506 CdEC flox KI mouse with Myh6-Cre-Prmt1 gRNA transgene (CdEC KI/Tg⁺) or without transgene
507 (CdEC KI/Tg⁻). (g) Morphogenic observation of hearts from 6-week-old CdEC KI/Tg⁺ and CdEC
508 KI/Tg⁻ mice. (h) Schematic representation of gRNA-Ddx4-CreERT2 donor plasmid DNA. Only the
509 region between two ITRs is described. (i) Observation of newborn CdEC KI mice with the
510 gRNA-Ddx4-CreERT2 transgene (CdEC KI/Tg⁺). (j) Results of HE-staining analysis of testes
511 removed from CdEC KI/Tg⁺ mice before and after tamoxifen injection. Arrowheads indicate
512 seminiferous tubules not containing sperm heads. (k) Percentage of seminiferous tubules without
513 sperm head in the testes from CdEC KI/Tg⁺ mice before and after tamoxifen injection. (l) Results of
514 the immunostaining analysis of testes from CdEC KI/Tg⁺ mice after tamoxifen injection using
515 anti-Cas9 and anti-GFR α 1 antibody.

516

517 **Figure 4 Generation of Tg mice using oocytes from C57BL6J and sperm from PWK strain**

518 (a) Schematic showing the timing of donor DNA microinjections relative to cell-cycle progression in
519 the mouse embryo. (b) Results of Southern blot analysis using DNA from E11.5 Tg embryo obtained

520 with a probe for the GFP region. DNA from WT mouse was used as a negative control. DNA from
521 GRR KI mouse was used as a positive control. (c) Copy number analysis of the transgenes using
522 DNA from E11.5 Tg embryo obtained by ddPCR with a probe for the GFP region. (d) Summary of
523 genome-wide distribution of the transgene insertion sites. (e) Summary of the transgene integration
524 sites. (f) Percentage of transgene insertion sites overlapping with H3K4me3 peaks. (g) An example
525 of a transgene insertion region overlapping with H3K4me3 peaks.

526 **References**

- 527 1. Tai, L. M., Maldonado Weng, J., LaDu, M. J. & Brady, S. T. Relevance of transgenic mouse
528 models for Alzheimer's disease. *Prog. Mol. Biol. Transl. Sci.* **177**, 1–48 (2021).
- 529 2. Lamprecht Tratar, U., Horvat, S. & Cemazar, M. Transgenic Mouse Models in Cancer Research.
530 *Front. Oncol.* **8**, 268 (2018).
- 531 3. Seita, Y. *et al.* Generation of Transgenic Cynomolgus Monkeys Overexpressing the Gene for
532 Amyloid- β Precursor Protein. *J. Alzheimers. Dis.* **75**, 45–60 (2020).
- 533 4. Skarnes, W. C. The identification of new genes: gene trapping in transgenic mice. *Curr. Opin.*
534 *Biotechnol.* **4**, 684–689 (1993).
- 535 5. Gu, B., Posfai, E. & Rossant, J. Efficient generation of targeted large insertions by
536 microinjection into two-cell-stage mouse embryos. *Nat. Biotechnol.* **36**, 632–637 (2018).
- 537 6. Mizuno, N. *et al.* Intra-embryo Gene Cassette Knockin by CRISPR/Cas9-Mediated Genome
538 Editing with Adeno-Associated Viral Vector. *iScience* **9**, 286–297 (2018).
- 539 7. Yoshimi, K. *et al.* ssODN-mediated knock-in with CRISPR-Cas for large genomic regions in
540 zygotes. *Nat. Commun.* **7**, 10431 (2016).
- 541 8. Jaenisch, R. & Mintz, B. Simian virus 40 DNA sequences in DNA of healthy adult mice derived
542 from preimplantation blastocysts injected with viral DNA. *Proc. Natl. Acad. Sci. U. S. A.* **71**,
543 1250–1254 (1974).
- 544 9. Gordon, J. W., Scangos, G. A., Plotkin, D. J., Barbosa, J. A. & Ruddle, F. H. Genetic
545 transformation of mouse embryos by microinjection of purified DNA. *Proc. Natl. Acad. Sci. U.*
546 *S. A.* **77**, 7380–7384 (1980).
- 547 10. Belizário, J. E., Akamini, P., Wolf, P., Strauss, B. & Xavier-Neto, J. New routes for transgenesis
548 of the mouse. *J. Appl. Genet.* **53**, 295–315 (2012).
- 549 11. Ikawa, M., Tanaka, N., Kao, W. W.-Y. & Verma, I. M. Generation of transgenic mice using
550 lentiviral vectors: a novel preclinical assessment of lentiviral vectors for gene therapy. *Mol.*
551 *Ther.* **8**, 666–673 (2003).
- 552 12. McClintock, B. The origin and behavior of mutable loci in maize. *Proc. Natl. Acad. Sci. U. S. A.*

- 553 **36**, 344–355 (1950).
- 554 13. Suster, M. L., Sumiyama, K. & Kawakami, K. Transposon-mediated BAC transgenesis in
555 zebrafish and mice. *BMC Genomics* **10**, 477 (2009).
- 556 14. Garrels, W. *et al.* Cytoplasmic injection of murine zygotes with Sleeping Beauty transposon
557 plasmids and minicircles results in the efficient generation of germline transgenic mice.
558 *Biotechnol. J.* **11**, 178–184 (2016).
- 559 15. Ding, S. *et al.* Efficient transposition of the piggyBac (PB) transposon in mammalian cells and
560 mice. *Cell* **122**, 473–483 (2005).
- 561 16. Ivics, Z. *et al.* Transposon-mediated genome manipulation in vertebrates. *Nat. Methods* **6**,
562 415–422 (2009).
- 563 17. Sunagawa, G. A. *et al.* Mammalian Reverse Genetics without Crossing Reveals Nr3a as a
564 Short-Sleeper Gene. *Cell Rep.* **14**, 662–677 (2016).
- 565 18. Dickinson, M. E. *et al.* High-throughput discovery of novel developmental phenotypes. *Nature*
566 **537**, 508–514 (2016).
- 567 19. Wei, T., Cheng, Q., Min, Y.-L., Olson, E. N. & Siegwart, D. J. Systemic nanoparticle delivery of
568 CRISPR-Cas9 ribonucleoproteins for effective tissue specific genome editing. *Nat. Commun.*
569 **11**, 3232 (2020).
- 570 20. Morita, S. *et al.* A Lipid Nanoparticle-Based Method for the Generation of Liver-Specific
571 Knockout Mice. *Int. J. Mol. Sci.* **24**, (2023).
- 572 21. Onuma, H., Sato, Y. & Harashima, H. Lipid nanoparticle-based ribonucleoprotein delivery for
573 in vivo genome editing. *J. Control. Release* **355**, 406–416 (2023).
- 574 22. Lee, B. *et al.* Nanoparticle delivery of CRISPR into the brain rescues a mouse model of fragile
575 X syndrome from exaggerated repetitive behaviours. *Nat Biomed Eng* **2**, 497–507 (2018).
- 576 23. Horii, T. *et al.* Efficient generation of conditional knockout mice via sequential introduction of
577 lox sites. *Sci. Rep.* **7**, 7891 (2017).
- 578 24. Carroll, K. J. *et al.* A mouse model for adult cardiac-specific gene deletion with CRISPR/Cas9.
579 *Proc. Natl. Acad. Sci. U. S. A.* **113**, 338–343 (2016).

- 580 25. Xiao, D. *et al.* CRISPR-mediated rapid generation of neural cell-specific knockout mice
581 facilitates research in neurophysiology and pathology. *Mol Ther Methods Clin Dev* **20**, 755–764
582 (2021).
- 583 26. Mizuno-Iijima, S. *et al.* Efficient production of large deletion and gene fragment knock-in mice
584 mediated by genome editing with Cas9-mouse Cdt1 in mouse zygotes. *Methods* **191**, 23–31
585 (2021).
- 586 27. Tanimoto, Y. *et al.* Zygote Microinjection for Creating Gene Cassette Knock-in and Flox
587 Alleles in Mice. *J. Vis. Exp.* (2022) doi:10.3791/64161.
- 588 28. Takeo, T. & Nakagata, N. Reduced glutathione enhances fertility of frozen/thawed C57BL/6
589 mouse sperm after exposure to methyl-beta-cyclodextrin. *Biol. Reprod.* **85**, 1066–1072 (2011).
- 590 29. Kaneko, T. & Mashimo, T. Simple Genome Editing of Rodent Intact Embryos by
591 Electroporation. *PLoS One* **10**, e0142755 (2015).
- 592 30. Yamagata, K. *et al.* Noninvasive visualization of molecular events in the mammalian zygote.
593 *Genesis* **43**, 71–79 (2005).
- 594 31. Ishitobi, H. *et al.* Flk1-GFP BAC Tg mice: an animal model for the study of blood vessel
595 development. *Exp. Anim.* **59**, 615–622 (2010).
- 596 32. Ishitobi, H. *et al.* Molecular basis for Flk1 expression in hemato-cardiovascular progenitors in
597 the mouse. *Development* **138**, 5357–5368 (2011).
- 598 33. Ochman, H., Gerber, A. S. & Hartl, D. L. Genetic applications of an inverse polymerase chain
599 reaction. *Genetics* **120**, 621–623 (1988).
- 600 34. Murata, K. *et al.* PRMT1 Deficiency in Mouse Juvenile Heart Induces Dilated Cardiomyopathy
601 and Reveals Cryptic Alternative Splicing Products. *iScience* **8**, 200–213 (2018).
- 602 35. Hasegawa, Y. *et al.* Novel ROSA26 Cre-reporter knock-in C57BL/6N mice exhibiting green
603 emission before and red emission after Cre-mediated recombination. *Exp. Anim.* **62**, 295–304
604 (2013).
- 605 36. Yoshida, J. *et al.* Chromatin states shape insertion profiles of the piggyBac, Tol2 and Sleeping
606 Beauty transposons and murine leukemia virus. *Sci. Rep.* **7**, 43613 (2017).

- 607 37. Zhang, B. *et al.* Allelic reprogramming of the histone modification H3K4me3 in early
608 mammalian development. *Nature* **537**, 553–557 (2016).
- 609 38. Sandoval-Villegas, N., Nurieva, W., Amberger, M. & Ivics, Z. Contemporary Transposon Tools:
610 A Review and Guide through Mechanisms and Applications of Sleeping Beauty, piggyBac and
611 Tol2 for Genome Engineering. *Int. J. Mol. Sci.* **22**, (2021).
- 612 39. Rostovskaya, M. *et al.* Transposon mediated BAC transgenesis via pronuclear injection of
613 mouse zygotes. *Genesis* **51**, 135–141 (2013).
- 614 40. Urschitz, J. *et al.* Helper-independent piggyBac plasmids for gene delivery approaches:
615 strategies for avoiding potential genotoxic effects. *Proc. Natl. Acad. Sci. U. S. A.* **107**,
616 8117–8122 (2010).
- 617 41. Marh, J. *et al.* Hyperactive self-inactivating piggyBac for transposase-enhanced pronuclear
618 microinjection transgenesis. *Proc. Natl. Acad. Sci. U. S. A.* **109**, 19184–19189 (2012).
- 619 42. Zhang, Y. *et al.* Expression of threonine-biosynthetic genes in mammalian cells and transgenic
620 mice. *Amino Acids* **46**, 2177–2188 (2014).
- 621 43. Bjork, B. C. *et al.* A transient transgenic RNAi strategy for rapid characterization of gene
622 function during embryonic development. *PLoS One* **5**, e14375 (2010).
- 623 44. Katter, K. *et al.* Transposon-mediated transgenesis, transgenic rescue, and tissue-specific gene
624 expression in rodents and rabbits. *FASEB J.* **27**, 930–941 (2013).
- 625 45. Zhao, L., Ng, E. T. & Koopman, P. A piggyBac transposon- and gateway-enhanced system for
626 efficient BAC transgenesis. *Dev. Dyn.* **243**, 1086–1094 (2014).
- 627 46. Eto, T. *et al.* Establishment of an integrated automated embryonic manipulation system for
628 producing genetically modified mice. *Sci. Rep.* **11**, 11770 (2021).
- 629 47. Horii, T., Morita, S., Kimura, M. & Hatada, I. Efficient generation of epigenetic disease model
630 mice by epigenome editing using the piggyBac transposon system. *Epigenetics Chromatin* **15**,
631 40 (2022).
- 632 48. Li, T. *et al.* Efficient Production of Fluorescent Transgenic Rats using the piggyBac Transposon.
633 *Sci. Rep.* **6**, 33225 (2016).

- 634 49. Jung, C. J. *et al.* Comparative Analysis of piggyBac, CRISPR/Cas9 and TALEN Mediated BAC
635 Transgenesis in the Zygote for the Generation of Humanized SIRPA Rats. *Sci. Rep.* **6**, 31455
636 (2016).
- 637 50. Jang, C.-W. & Behringer, R. R. Transposon-mediated transgenesis in rats. *CSH Protoc.* **2007**,
638 db.prot4866 (2007).
- 639 51. Yum, S.-Y. *et al.* Efficient generation of transgenic cattle using the DNA transposon and their
640 analysis by next-generation sequencing. *Sci. Rep.* **6**, 27185 (2016).
- 641 52. Kwon, D.-H., Gim, G.-M., Eom, K.-H., Lee, J.-H. & Jang, G. Application of transposon
642 systems in the transgenesis of bovine somatic and germ cells. *BMC Vet. Res.* **18**, 156 (2022).
- 643 53. Shakweer, W. M. E., Krivoruchko, A. Y., Dessouki, S. M. & Khattab, A. A. A review of
644 transgenic animal techniques and their applications. *J. Genet. Eng. Biotechnol.* **21**, 55 (2023).
- 645 54. Van Eenennaam, A. L., De Figueiredo Silva, F., Trott, J. F. & Zilberman, D. Genetic
646 Engineering of Livestock: The Opportunity Cost of Regulatory Delay. *Annu Rev Anim Biosci* **9**,
647 453–478 (2021).

Figure 1

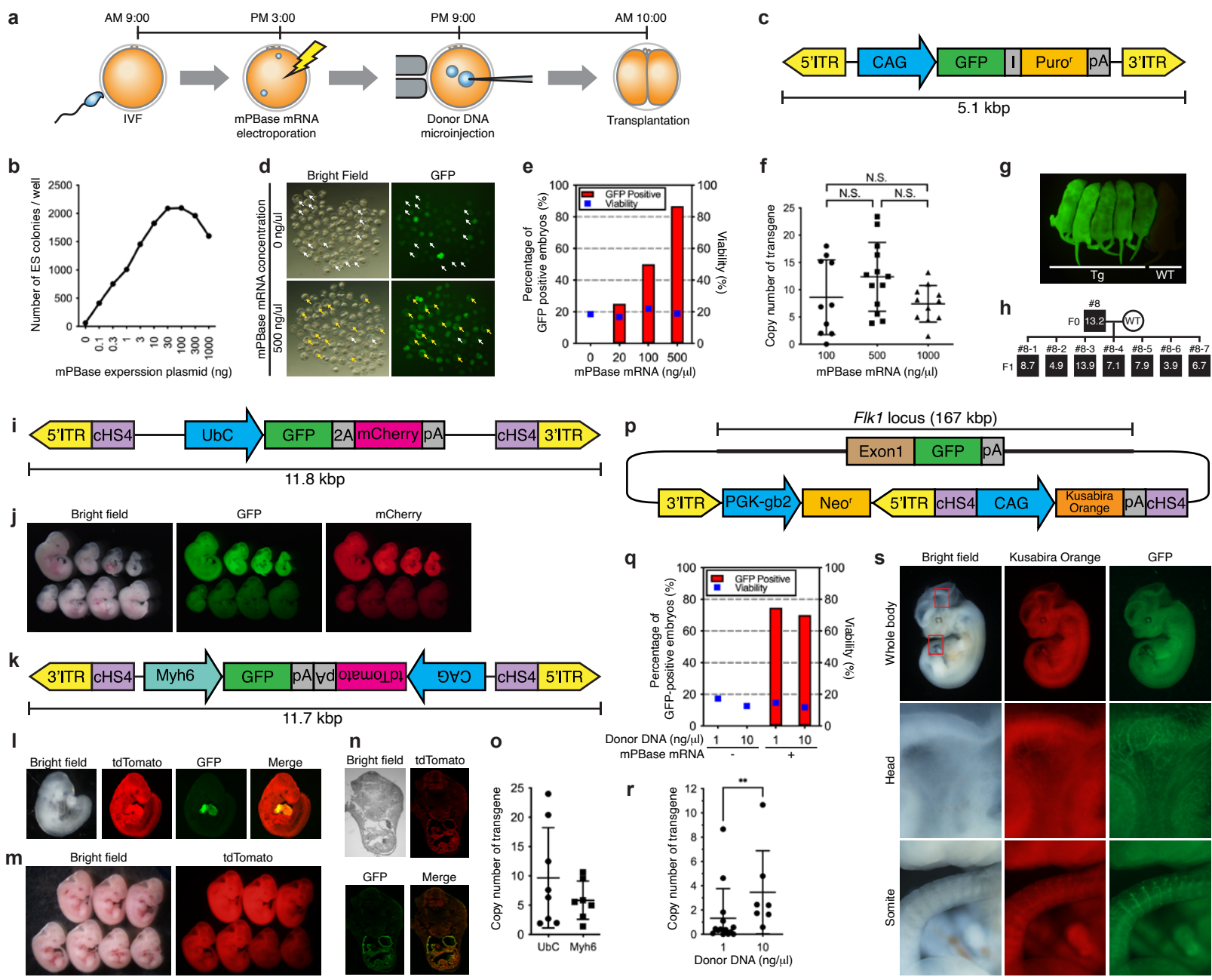
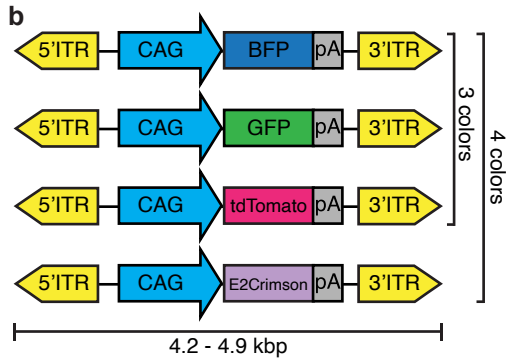
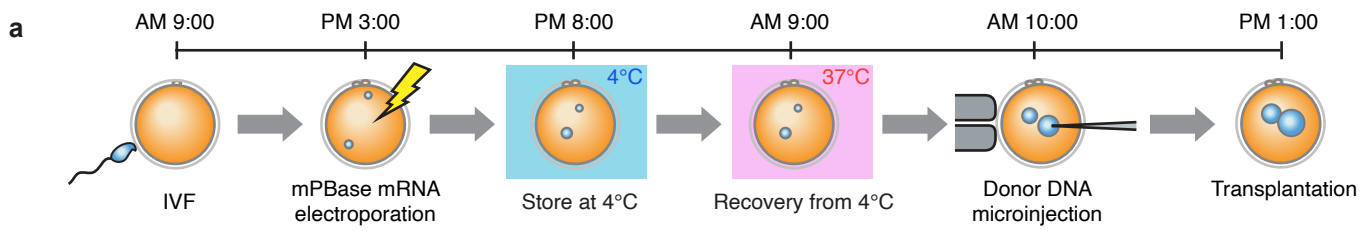


Figure 2



c

Embryo No.	3 colors donor DNA												4 colors donor DNA				
	1	2	3	4	5	6	7	8	9	10	11	12	1	2	3	4	
BFP	+	+	+	+	+	+	-	+	-	+	+	+	+	+	+	+	-
GFP	+	+	+	+	+	-	-	+	+	+	+	+	+	+	+	+	-
tdTomato	+	+	+	+	+	-	-	+	+	+	+	+	+	+	+	+	-
E2Crimson	-	-	-	-	-	-	-	-	-	-	-	-	-	+	+	+	-

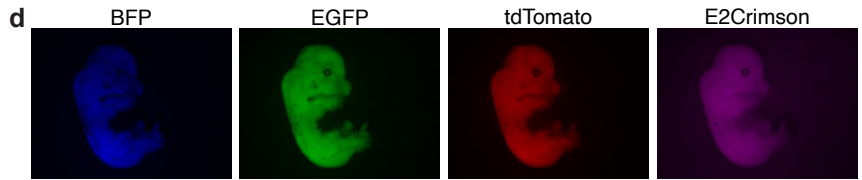


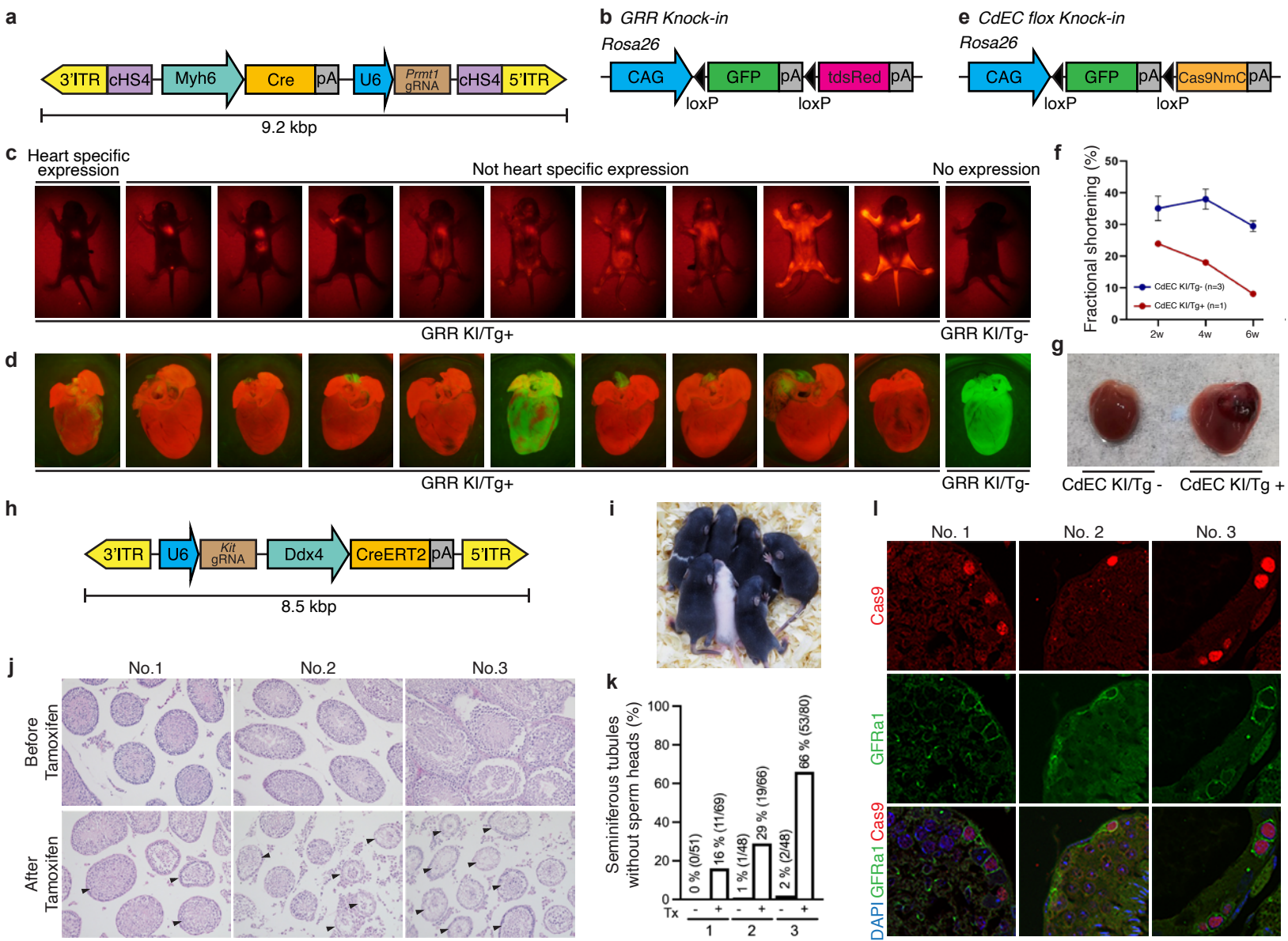
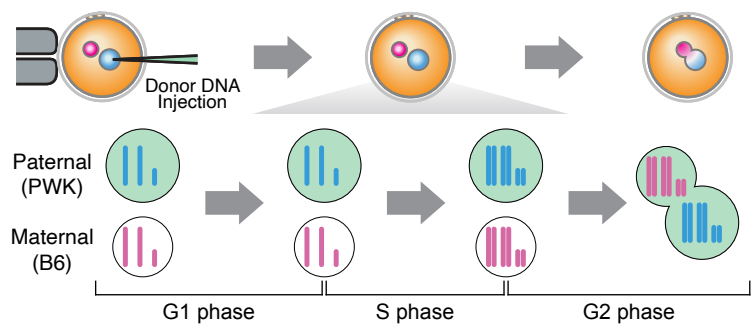
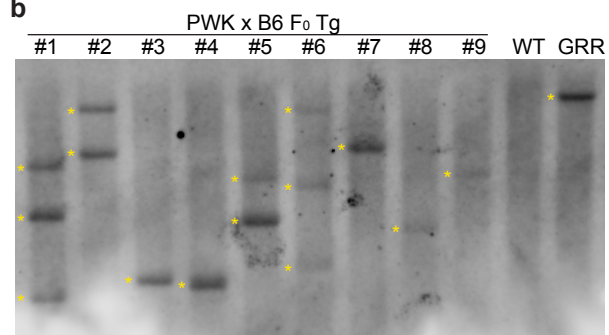
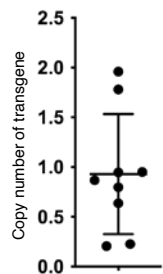
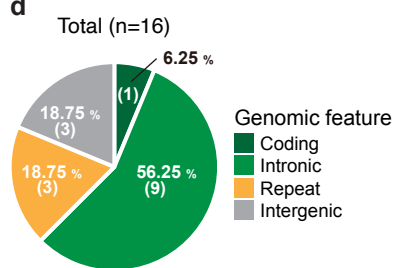
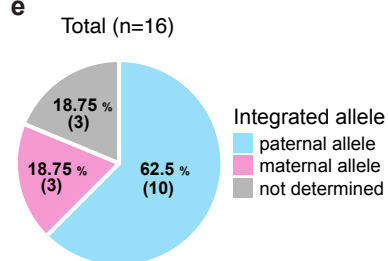
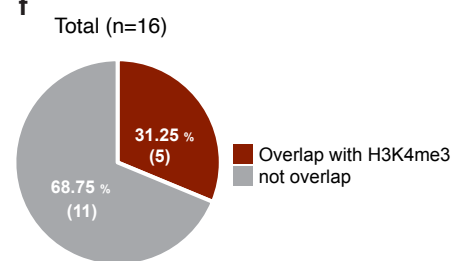
Figure 3

Figure 4**a****b****c****d****e****f****g**